Identifying and Constructing Complex Magnon Band Topology

Alberto Corticelli, Roderich Moessner, and Paul A. McClarty
Max Planck Institute for the Physics of Complex Systems, Nöthnitzer Strasse 38, 01187 Dresden, Germany

(Received 28 April 2022; revised 20 December 2022; accepted 28 April 2023; published 19 May 2023)

Magnetically ordered materials tend to support bands of coherent propagating spin wave, or magnon, excitations. Topologically protected surface states of magnons offer a new path toward coherent spin transport for spintronics applications. In this work we explore the variety of topological magnon band structures and provide insight into how to efficiently identify topological magnon bands in materials. We do this by adapting the topological quantum chemistry approach that has used constraints imposed by time reversal and crystalline symmetries to enumerate a large class of topological electronic bands. We show how to identify physically relevant models of gapped magnon band topology by using so-called decomposable elementary band representations, and in turn discuss how to use symmetry data to infer the presence of exotic symmetry enforced nodal topology.

DOI: 10.1103/PhysRevLett.130.206702

Introduction.—There have been considerable efforts in the last few years to provide a taxonomy of nontrivial topological band structures enforced or allowed by time reversal and crystalline symmetries [1–15]. This work has brought powerful new concepts that tie crystal and magnetic structures to band topology. At the same time these ideas provide efficient methods to efficiently search for topological materials resulting in a vast database of *ab initio* driven predictions of new electronic topological materials [16,17]. Such materials include gapless and gapped bulk topological matter with protected boundary states and anomalous transport properties. The culmination of these efforts to classify band topology based on symmetry and to use symmetry data to diagnose topological bands is called topological quantum chemistry (TQC) [8,14].

In a similar time frame, there has been increasing interest in exploring the role of band topology in *magnetic* excitations and how it affects the properties of magnetic materials [18–20]. The pioneering work in this area has mainly been in devising physically well-motivated models of magnon band topology such as Chern insulators and Weyl magnons [21–35]. This has inspired early experimental efforts to characterize magnon topology in materials [36–41]. All this work has gone hand in hand with the exploration of unusual experimental signatures originating from the geometry and topology of magnon bands [38,39,42–51]. On the horizon, there are exciting potential developments to be made detecting and manipulating topological magnon boundary states [52–55].

In this Letter, we show that the TQC approach can be adapted to magnon band topology, providing a classification of *symmetry-determined* topological bands in spin wave Hamiltonians. The ideas can be used to diagnose magnon topology on one hand, and on the other to build models and identify candidate topological magnon materials. The physical foundation for this work is that topological bands by definition cannot be built from a Wannier basis, a set of exponentially localized orbitals, while preserving all underlying symmetries. Topological quantum chemistry rests on an enumeration of all possible Wannierizable band structures through so-called elementary band representations (EBRs), to be described in more detail below so that, essentially by elimination, one may establish whether some set of bands is topologically nontrivial.

Ab initio methods are central to TQC. The closest analog in widespread use to study magnetic excitations is linear spin wave theory which is based on an expansion, to quadratic order, of the spins in fluctuations around some magnetic structure. The goal of this Letter is to show how to pass from elementary symmetry information—the crystal structure and the magnetic order—to linear spin wave models with nontrivial topology.

Our starting point is to establish how crystal and time reversal symmetries are implemented within linear spin wave theory. In contrast to electronic systems, the band structures of interest emerge from an effective exchange Hamiltonian. We describe how this Hamiltonian, in conjunction with the minimal energy magnetic structure, fixes the symmetries of the problem. These are encoded in some magnetic space group [56]. We then outline how to build band representations for magnons starting from the local

moments on each magnetic site giving a complete table of all site symmetry groups compatible with magnetic order. Band representations minimally encode symmetry information in the magnon band structure. With these ingredients, we are in a position to identify constraints that magnons place on the possible symmetry data and hence on the possible topological bands. In particular, it turns out that magnons in systems with *significant spin-orbit coupling* form a subset of all electronic topological bands.

With these foundations, we then show, first in general and then through a series of examples, how to use symmetry information alone to build exchange models whose elementary excitations have nontrivial gapped and nodal magnon topology and to identify candidate materials. Examples include Chern bands, antiferromagnetic topological insulators, and threefold and sixfold nodal points. Crucially, our workflow can be straightforwardly reversed, to diagnose nontrivial topology from spin wave fits to experimental data.

EBRs and topology.—Before getting into the specifics for magnons, we give a lightning introductory review of TQC. We refer the reader to the Supplemental Material [57] for more technical details that will not, however, be necessary to appreciate the remainder of this Letter.

The essential symmetry ingredients of TQC are nothing more than the symmetry group G_M of the magnetic structure and the Wyckoff positions of the magnetic ions that appear in any structural refinement of a magnetic material. The group G_M is generally one of the magnetic space groups that encodes combinations of crystallographic point group symmetries, lattice translations, time reversal symmetry, and perhaps nonsymmorphic elements. To each Wyckoff position $\boldsymbol{q}$, we may assign a site symmetry group (SSG) $G_{\boldsymbol{q}}$ defined as the subgroup of G_M that leaves the site invariant. This is generally isomorphic to a magnetic point group.

We then need to include some information about the underlying lattice degrees of freedom—the nature of the atomic orbitals. These necessarily transform under some representation of $G_{\boldsymbol{q}}$. Following Zak, from these representations of the magnetic SSG we may arrive at a representation of the full G_M group by the standard process of *induction* [66]. The result is a so-called band representation (BR). The BR is a momentum space representation of all elements of G_M that contains information about the connectivity of the bands and the topology. To connect to topology we define EBRs to be BRs that are not unitarily equivalent to a direct sum of two or more BRs. These hold a distinguished place in relation to topology because they are the elementary units from which all Wannierizable band structures can be built for a given symmetry group. Any set of bands that cannot be built from EBRs is necessarily topological overall. All EBRs for all magnetic space groups have been tabulated—each one characterized by eigenvalues of all symmetry operations at high symmetry momenta. For all 1651 magnetic space groups, there are roughly 20000 EBRs. In order to diagnose topological bands, one should in principle determine whether each energetically isolated set of bands can be written as a direct sum of EBRs with non-negative integer coefficients. If so, the bands are trivial. If not, they are symmetry-determined topological gapped bands. A more fine-grained determination of the nature of the topology then requires further analysis. On the other hand, symmetry enforced nodal topological bands can be read off directly from the dimension greater than one irreducible representation at high symmetry points, lines, and planes.

Magnons and symmetry.—Building on the principles behind TQC we now discuss the ideas in relation to magnons. In this work we are mainly interested in crystalline solids with localized magnetic moments and nonvanishing local dipolar order parameter $\langle S_i^\alpha \rangle$ for site i and component α. The magnon or spin wave excitations are the transverse fluctuations of the local ordered moments. We restrict our attention to the typical case where these form coherent propagating bands. This means we neglect the role of multimagnon states and possible interesting questions of novel topology [67] and fragility that arise from such states. We also neglect magnetic excitations beyond the ground state multiplet that could be handled within a multiboson formalism (see, e.g., Ref. [38]) to which TQC ideas may also be applied.

The symmetries of the magnon bands are descended from those of the magnetic Hamiltonian H_M considered to be composed of exchange couplings, dipolar couplings [68–71], single ion anisotropies, and perhaps an external magnetic field. The magnetic order breaks the symmetries of the magnetic Hamiltonian down to a subgroup. It is important to note that the relevant symmetry groups for magnons are single valued (i.e., acting on normal vectors) because the bands are spinless or bosonic. These are the groups that are relevant to weakly spin-orbit coupled electronic systems. However, in the context of magnons, these groups are relevant to the case where the moments and the spatial transformations are locked, which can only happen when spin-orbit coupling at the microscopic level is significant. The spin-orbit coupling is reflected in the appearance of anisotropies in the magnetic Hamiltonian. We implicitly assume that all symmetry-allowed bilinear exchange couplings are present for a given crystallographic group. In such a context we implicitly take into account specific important anisotropy terms like the Dzyaloshinskii-Moriya interaction or symmetric off-diagonal exchange. However as is well known, there are many cases where the magnetic Hamiltonian has discrete or continuous spin rotation symmetries. In such cases, magnetic order may lead to residual symmetries described by the spin-space groups [58,72–74]. Topological quantum chemistry applied to such groups is beyond the scope of this work. We consider the case where these residual symmetries

are those of a magnetic space group G_M with n_S sublattices in the magnetic primitive cell leading to n_S bands considered to be computed from linear spin wave theory based on Hamiltonian $H_{\mathrm{LSW}} = (S/2)\sum_{\boldsymbol{k}} \hat{\Upsilon}^{\dagger}(\boldsymbol{k})\boldsymbol{M}(\boldsymbol{k})\hat{\Upsilon}(\boldsymbol{k})$ where the transformation properties of $2n_S$ component $\hat{\Upsilon}(\boldsymbol{k})$ can be inferred from the transformations of the $S_i^{\pm}$ transverse spin components in a frame where S^z is the direction of the ordered moment. For reference, explicit formulas are given in the Supplemental Material [57].

The transverse spin components in the local quantization frame $S_i^{\pm}$ are the analogs to local Wannier orbitals in building band representations. With this ingredient, to build a magnon band representation, only *two* further pieces of information are needed: the magnetic space group G_M and the Wyckoff positions $\boldsymbol{q}$ of the magnetic ions. We provide the list of all topological gapped and nodal magnon band representations appropriate to magnons from the full TQC tabulations in the Supplemental Material [57].

In the remainder of this Letter, we give concrete examples of how to use the tabulated EBRs to build models of topological magnons. We take two main routes. The first is to focus on cases where the symmetry information about band connectivity allows EBRs to split up into disconnected bands. By definition at least one of the resulting bands must be topological. Our second focus will be on nodal topology. Several models are known with Dirac and Weyl magnon touching points [18]. But symmetry can enforce higher order degeneracies three-, four-, and sixfold degeneracies, and we show how to build models with such degeneracies.

Magnon topology from decomposable EBRs.—To build models of decomposable EBRs we focus on cases where the magnetic ions live on *maximal* Wyckoff positions, i.e., positions of maximal magnetic point group symmetry for a given G_M. These are distinguished by the fact that BRs induced from such sites are themselves EBRs and not composites of EBRs (apart from some well-understood exceptional cases). We give a complete table of decomposable EBRs that can be obtained from maximal Wyckoff positions and the allowed SSGs organized by magnetic space group and Wyckoff position [57]. The utility of this table is that one may couple moments living on such Wyckoff positions and be sure that there will be nontrivial topology in the resulting magnon bands provided free parameters are tuned to avoid accidental degeneracies and provided the number of free parameters is adequate to reduce the symmetries to the required G_M. This approach is a highly efficient means to build models of magnon topology and contrasts to generic cases of nontrivial topology where, in practice, one should compute so-called symmetry indicators as a function of free couplings to diagnose the topology.

We reverse the usual logic to show how the model might have been inferred from the tabulated decomposable EBRs. Let us consider magnetic space group $F\bar{3}1m'$ (162.77 in the Belov–Neronova–Smirnova (BNS) convention) and Wyckoff position $2c$ corresponding to honeycomb layers. The magnetic site symmetry group is $32'$, and the moments are perpendicular to the honeycomb planes. The orbital basis on the $2c$ positions $(J_{\boldsymbol{q}}^{+}, J_{\boldsymbol{q}}^{-})$ transforms under the ${}^1E + {}^2E$ irreducible representations (irreps) of the SSG. Consultation of tables in the Supplemental Material [57] or on the Bilbao crystallographic server [59,60] reveals that induction to the full space group yields a single EBR that is decomposable into two bands. From symmetry alone we have therefore inferred the presence of nontrivial magnon band topology. A guide to using the Bilbao tables is given in the Supplemental Material [57].

With this established, we may now build a model hosting the decomposable EBR and further characterize the nature of the topology. To do this, one should write down couplings between the magnetic moments that both stabilize the required magnetic structure and respect the resulting magnetic space group symmetries. To respect both conditions, we compute all exchange couplings allowed by symmetry. To nearest neighbor these are the Heisenberg, Kitaev, Γ, and Γ' terms [33,75]. Kitaev and Heisenberg interactions are sufficient to respect $F\bar{3}1m'$, and a magnetic field may be applied along [111] to stabilize the structure if necessary. A linear spin wave calculation then reveals two propagating magnon bands with a gap between them. For decomposable EBRs the topology is not necessarily symmetry indicated but it turns out that the C_3 symmetry indicator formula [3] for the Chern number characterizes the topology in this case revealing two magnon bands with Chern numbers ± 1, the order depending on the sign of the Kitaev exchange [57].

We now sketch another example of gapped band topology working from the table of decomposable EBRs but this time without reference to an example already in the literature. Consider the tetragonal space group $P4$ (No. 75.1, a type I MSG) with two sublattice Wyckoff position $2c$ and irreps $2B$ for the transverse spin components, which again leads to a single decomposable EBR. We compute all symmetry-allowed exchange couplings for first up to fourth nearest neighbors and choose some set of couplings that stabilizes the required magnetic structure. The linear spin wave spectrum has two dispersive gapped bands, and the Chern number can, once again, be computed from a symmetry indicator formula,

$$i^C = \prod_n \xi_n(\Gamma)\xi_n(M)\zeta_n(X), \tag{1}$$

where C is the Chern number of the n band(s), while $\xi(\boldsymbol{k})$ and $\zeta(\boldsymbol{k})$ are the eigenvalues respectively of C_4 and C_2. Figure 1 shows the lattice structure and the band structure with the eigenvalues indicated. The computed Chern numbers are ± 1.

The method is not restricted to diagnosing Chern bands as we show now with a third example. We take space group

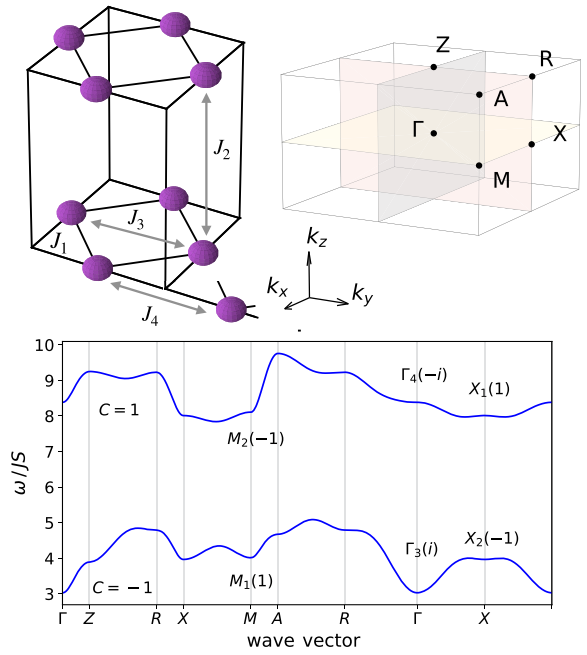

FIG. 1. Figure showing the magnetic sublattices of space group 75 Wyckoff position 2c and the accompanying Brillouin zone. The lower panel shows magnon dispersion relations along high symmetry directions with the C_2 and C_4 eigenvalues given according to the symmetry indicator formula Eq. (1).

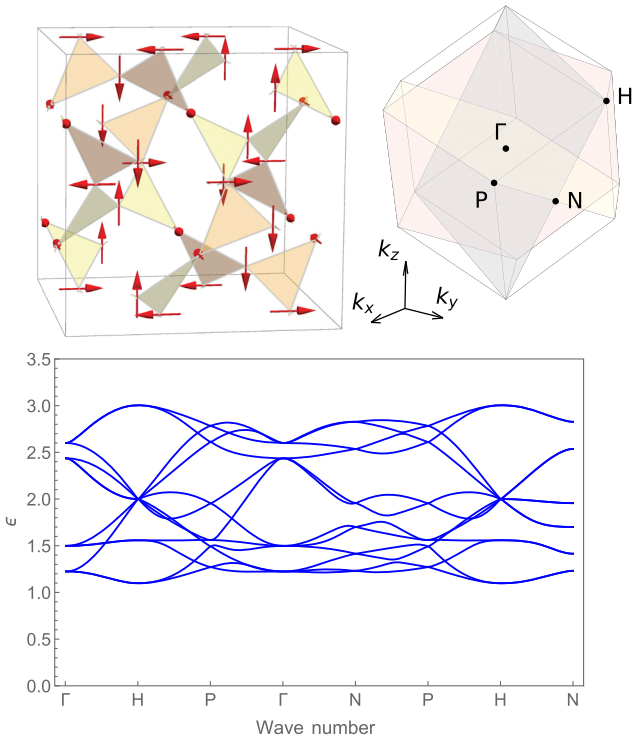

FIG. 2. Magnetic structure on the garnet hyperkagome lattice with 230.148 magnetic space group symmetry (top left) and (right) the Brillouin zone with high symmetry points indicated. Bottom: spin wave spectrum with multifold magnons at Γ and H.

P_c6/mcc (192.252) and Wyckoff position 4c which has SSG $-6m'2'$. This corresponds to an AA stacked honeycomb lattice with moments perpendicular to the plane that are ferromagnetically ordered in the plane and antiferromagnetically aligned between planes. Crucially this system is symmetric under time reversal times a translation that maps one layer to the next. The two magnon bands within each layer each carry a net Chern number which reverses between layers. One may show [57] that the coupled four magnon bands correspond to a single EBR that is decomposable. The result is an antiferromagnetic topological insulator that can be realized with an anisotropic exchange model for the in-plane moments with Heisenberg exchange between the layers. An explicit calculation of the band structure is provided for reference in the Supplemental Material [57] (see also Ref. [61]).

Symmetry enforced nodal topology.—In this part, we turn our attention to nodal topology focusing on exotic degeneracies that are enforced by symmetry: magnonic analogs of multifold fermion degeneracies [76,77]. In the Supplemental Material [57] we show how to use the Bilbao tables [59,60] to establish symmetry-enforced degeneracies and give extensive tables of such degeneracies for magnons [57]. Here we show how to build models based on the symmetry information.

The first example is for magnetic space group 227.131—a type III group—and Wyckoff position 16d corresponding to all-in-all-out (AIAO) order on the A site of pyrochlore materials as realized in $Nd_2M_2O_7$ (M = Sn, Hf, Ir, Zr) [78–82], $Sm_2Ir_2O_7$ [83], $Eu_2Ir_2O_7$ [84], and $Cd_2Os_2O_7$ [85], as well as FeF_3 [86]. The single-valued symmetry group enforces a threefold degenerate point at Γ [59,60]. A simple model consists of antiferromagnetic Heisenberg coupling with a weak $\langle 111 \rangle$ Ising anisotropy that lifts the degeneracy of the Heisenberg model [87] in favor of the AIAO structure. A linear spin wave calculation [57] reveals four dispersive modes with a spectral gap and the threefold degenerate point at Γ. The existence of this quadratically dispersing threefold point has previously been noted in Ref. [62] as a parent state for Weyl fermions upon symmetry breaking with strain or an applied magnetic field.

For our next example, inspection of the table of degeneracies [57] reveals sixfold degeneracies for magnetic space group 230.148 and Wyckoff position 24c. The nearest neighbor exchange leads to two decoupled 12-site magnetic sublattices of corner-sharing triangles—a hyperkagome structure that arises on the R sites of garnets with chemical formula $R_3M_5O_{12}$. The magnetic structures have moments oriented along three cubic directions on each triangular face as in Fig. 2. This structure is observed in the material $Dy_3M_5O_{12}$ (M = Al, Ga) [88–90]. The symmetry-allowed nearest neighbor couplings necessary to stabilize this structure are in the Supplemental Material [57] and with an additional antiferromagnetic Heisenberg exchange between the two hyperkagome sublattices we obtain a spin

wave spectrum as in Fig. 2. This has several symmetry enforced multifold bosonic points including four threefold points at Γ with quadratic dispersion and one sixfold point at H on the zone boundary with linear dispersion that is a doubled spin-1 Weyl point.

Discussion.—The classification of topological materials based on crystalline and time reversal symmetries is at a mature stage. In the foregoing we have connected the symmetry-based classification scheme based on elementary band representations to topological magnons. To do this, we showed how symmetries are inherited by magnons from those of the underlying exchange Hamiltonian and indicated how to build band representations for magnons. We have given conditions for the existing tables of EBRs to be applicable to topological magnons. We have shown through several examples that one can use the computed decomposable elementary band representations for single-valued magnetic space groups to build realistic, non-fine-tuned models of topological magnon band structures.

We have also used tabulated symmetry-enforced degeneracies as a guide to building exchange models of exotic nodal topology such as sixfold degenerate touching points. Moreover, we have used the magnon band representation tables to search for topological features among the commensurate materials on the MAGNDATA database of magnetic materials [63]. Importantly this database lists materials by magnetic structure alone with no further information about magnons. The power of the TQC method is evident in the predictions one can make about their magnon topology based purely on symmetry [57].

Magnons provide an excellent platform to explore the interplay of magnetic symmetries and topology in conjunction with inelastic neutron scattering. Furthermore topological magnonic surface states confined within a few Angstroms are generically robust against disorder and highly tunable, rendering possible applications including various topological spin wave devices like wave guides, spin wave diodes, beam splitters, and interferometers [25,54,91] In addition to model building and experimental discovery within the framework laid out here, important open avenues are to explore magnon topology beyond the decomposable EBR paradigm within the TQC framework and to extend TQC to the spin-space groups that are applicable to Heisenberg models among other systems.

P. M. acknowledges useful discussions with Alexei Andreanov on magnetism in the garnets. This work was in part supported by the Deutsche Forschungsgemeinschaft under Grant No. SFB 1143 (Project ID No. 247310070) and the cluster of excellence ct.qmat (EXC 2147, Project ID No. 390858490).

[1] S. Ryu, A. P. Schnyder, A. Furusaki, and A. W. Ludwig, New J. Phys. **12**, 065010 (2010).
[2] Q.-R. Xu, V. P. Flynn, A. Alase, E. Cobanera, L. Viola, and G. Ortiz, Phys. Rev. B **102**, 125127 (2020).
[3] C. Fang, M. J. Gilbert, and B. A. Bernevig, Phys. Rev. B **86**, 115112 (2012).
[4] S. A. Parameswaran, A. M. Turner, D. P. Arovas, and A. Vishwanath, Nat. Phys. **9**, 299 (2013).
[5] H. Watanabe, H. C. Po, A. Vishwanath, and M. Zaletel, Proc. Natl. Acad. Sci. U.S.A. **112**, 14551 (2015).
[6] H. C. Po, H. Watanabe, M. P. Zaletel, and A. Vishwanath, Sci. Adv. **2**, e1501782 (2016).
[7] H. Watanabe, H. C. Po, M. P. Zaletel, and A. Vishwanath, Phys. Rev. Lett. **117**, 096404 (2016).
[8] B. Bradlyn, L. Elcoro, J. Cano, M. G. Vergniory, Z. Wang, C. Felser, M. I. Aroyo, and B. A. Bernevig, Nature (London) **547**, 298 (2017).
[9] J. Kruthoff, J. de Boer, J. van Wezel, C. L. Kane, and R.-J. Slager, Phys. Rev. X **7**, 041069 (2017).
[10] H. Watanabe, H. C. Po, and A. Vishwanath, Sci. Adv. **4**, eaat8685 (2018).
[11] J. Cano, B. Bradlyn, Z. Wang, L. Elcoro, M. G. Vergniory, C. Felser, M. I. Aroyo, and B. A. Bernevig, Phys. Rev. B **97**, 035139 (2018).
[12] Z. Song, T. Zhang, Z. Fang, and C. Fang, Nat. Commun. **9**, 3530 (2018).
[13] Z. Song, T. Zhang, and C. Fang, Phys. Rev. X **8**, 031069 (2018).
[14] L. Elcoro, B. J. Wieder, Z. Song, Y. Xu, B. Bradlyn, and B. A. Bernevig, Nat. Commun. **12**, 5965 (2021).
[15] Y. Xu, L. Elcoro, Z.-D. Song, B. J. Wieder, M. G. Vergniory, N. Regnault, Y. Chen, C. Felser, and B. A. Bernevig, Nature (London) **586**, 702 (2020).
[16] M. G. Vergniory, L. Elcoro, C. Felser, N. Regnault, B. A. Bernevig, and Z. Wang, Nature (London) **566**, 480 (2019).
[17] Topological materials database, https://topologicalquantum-chemistry.org/.
[18] P. A. McClarty, Annu. Rev. Condens. Matter Phys. **13**, 171 (2022).
[19] V. Bonbien, F. Zhuo, A. Salimath, O. Ly, A. Abbout, and A. Manchon, J. Phys. D **55**, 103002 (2021).
[20] M. Malki and G. Uhrig, Europhys. Lett. **132**, 20003 (2020).
[21] L. Zhang, J. Ren, J.-S. Wang, and B. Li, Phys. Rev. B **87**, 144101 (2013).
[22] R. Shindou, J.-i. Ohe, R. Matsumoto, S. Murakami, and E. Saitoh, Phys. Rev. B **87**, 174402 (2013).
[23] R. Shindou, R. Matsumoto, S. Murakami, and J.-i. Ohe, Phys. Rev. B **87**, 174427 (2013).
[24] A. Mook, J. Henk, and I. Mertig, Phys. Rev. B **94**, 174444 (2016).
[25] A. Mook, J. Henk, and I. Mertig, Phys. Rev. B **91**, 174409 (2015).
[26] J. Romhányi, K. Penc, and R. Ganesh, Nat. Commun. **6**, 6805 (2015).
[27] A. Mook, J. Henk, and I. Mertig, Phys. Rev. B **99**, 014427 (2019).
[28] A. Mook, J. Henk, and I. Mertig, Phys. Rev. B **89**, 134409 (2014).
[29] A. Mook, J. Henk, and I. Mertig, Phys. Rev. B **90**, 024412 (2014).
[30] S. A. Díaz, J. Klinovaja, and D. Loss, Phys. Rev. Lett. **122**, 187203 (2019).

[31] A. Roldán-Molina, A. S. Nunez, and J. Fernández-Rossier, New J. Phys. **18**, 045015 (2016).
[32] S. A. Owerre, J. Phys. Condens. Matter **28**, 386001 (2016).
[33] P. A. McClarty, X.-Y. Dong, M. Gohlke, J. G. Rau, F. Pollmann, R. Moessner, and K. Penc, Phys. Rev. B **98**, 060404(R) (2018).
[34] F.-Y. Li, Y.-D. Li, Y. B. Kim, L. Balents, Y. Yu, and G. Chen, Nat. Commun. **7**, 12691 (2016).
[35] A. Mook, J. Henk, and I. Mertig, Phys. Rev. Lett. **117**, 157204 (2016).
[36] P. McClarty, F. Krüger, T. Guidi, S. Parker, K. Refson, A. Parker, D. Prabhakaran, and R. Coldea, Nat. Phys. **13**, 736 (2017).
[37] B. Yuan, I. Khait, G.-J. Shu, F. C. Chou, M. B. Stone, J. P. Clancy, A. Paramekanti, and Y.-J. Kim, Phys. Rev. X **10**, 011062 (2020).
[38] M. Elliot, P. A. McClarty, D. Prabhakaran, R. D. Johnson, H. C. Walker, P. Manuel, and R. Coldea, Nat. Commun. **12**, 3936 (2021).
[39] A. Scheie, P. Laurell, P. A. McClarty, G. E. Granroth, M. B. Stone, R. Moessner, and S. E. Nagler, Phys. Rev. Lett. **128**, 097201 (2022).
[40] A. Scheie, P. Laurell, P. A. McClarty, G. E. Granroth, M. B. Stone, R. Moessner, and S. E. Nagler, Phys. Rev. B **105**, 104402 (2022).
[41] T. Weber, D. M. Fobes, J. Waizner, P. Steffens, G. S. Tucker, M. Böhm, L. Beddrich, C. Franz, H. Gabold, R. Bewley, D. Voneshen, M. Skoulatos, R. Georgii, G. Ehlers, A. Bauer, C. Pfleiderer, P. Böni, M. Janoschek, and M. Garst, Science **375**, 1025 (2022).
[42] Y. Onose, T. Ideue, H. Katsura, Y. Shiomi, N. Nagaosa, and Y. Tokura, Science **329**, 297 (2010).
[43] H. Katsura, N. Nagaosa, and P. A. Lee, Phys. Rev. Lett. **104**, 066403 (2010).
[44] R. Matsumoto and S. Murakami, Phys. Rev. Lett. **106**, 197202 (2011).
[45] R. Matsumoto and S. Murakami, Phys. Rev. B **84**, 184406 (2011).
[46] R. Matsumoto, R. Shindou, and S. Murakami, Phys. Rev. B **89**, 054420 (2014).
[47] S. Murakami and A. Okamoto, J. Phys. Soc. Jpn. **86**, 011010 (2016).
[48] Y. Kasahara, K. Sugii, T. Ohnishi, M. Shimozawa, M. Yamashita, N. Kurita, H. Tanaka, J. Nasu, Y. Motome, T. Shibauchi *et al.*, Phys. Rev. Lett. **120**, 217205 (2018).
[49] Y. Kasahara, T. Ohnishi, Y. Mizukami, O. Tanaka, S. Ma, K. Sugii, N. Kurita, H. Tanaka, J. Nasu, Y. Motome *et al.*, Nature (London) **559**, 227 (2018).
[50] R. Hentrich, M. Roslova, A. Isaeva, T. Doert, W. Brenig, B. Büchner, and C. Hess, Phys. Rev. B **99**, 085136 (2019).
[51] S. Shivam, R. Coldea, R. Moessner, and P. McClarty, arXiv:1712.08535.
[52] J. Feldmeier, W. Natori, M. Knap, and J. Knolle, Phys. Rev. B **102**, 134423 (2020).
[53] D. Malz, J. Knolle, and A. Nunnenkamp, Nat. Commun. **10**, 3937 (2019).
[54] A. Rückriegel, A. Brataas, and R. A. Duine, Phys. Rev. B **97**, 081106(R) (2018).
[55] A. Mitra, A. Corticelli, P. Ribeiro, and P. A. McClarty, Phys. Rev. Lett. **130**, 066701 (2023).
[56] A. P. Cracknell, *Magnetism in Crystalline Materials: Applications of the Theory of Groups of Cambiant Symmetry* (Pergamon, Oxford, 1975).
[57] See Supplemental Material at http://link.aps.org/supplemental/10.1103/PhysRevLett.130.206702 for further details and additional supporting data, which includes Refs. [14,15,33,58–65].
[58] A. Corticelli, R. Moessner, and P. A. McClarty, Phys. Rev. B **105**, 064430 (2022).
[59] M. I. Aroyo, J. M. Perez-Mato, C. Capillas, E. Kroumova, S. Ivantchev, G. Madariaga, A. Kirov, and H. Wondratschek, Z. Kristallogr.—Cryst. Mater. **221**, 15 (2006).
[60] M. I. Aroyo, A. Kirov, C. Capillas, J. M. Perez-Mato, and H. Wondratschek, Acta Crystallogr. Sect. A **62**, 115 (2006).
[61] H. Kondo and Y. Akagi, Phys. Rev. Lett. **127**, 177201 (2021).
[62] S.-K. Jian and W. Nie, Phys. Rev. B **97**, 115162 (2018).
[63] S. V. Gallego, J. M. Perez-Mato, L. Elcoro, E. S. Tasci, R. M. Hanson, K. Momma, M. I. Aroyo, and G. Madariaga, J. Appl. Crystallogr. **49**, 1750 (2016).
[64] C. Bradley and A. Cracknell, *The Mathematical Theory of Symmetry in Solids: Representation Theory for Point Groups and Space Groups* (Oxford University Press, New York, 2009).
[65] D. G. Joshi, Phys. Rev. B **98**, 060405(R) (2018).
[66] J. Zak, Phys. Rev. B **23**, 2824 (1981).
[67] P. A. McClarty and J. G. Rau, Phys. Rev. B **100**, 100405(R) (2019).
[68] J. R. Eshbach and R. W. Damon, Phys. Rev. **118**, 1208 (1960).
[69] A. V. Chumak, A. A. Serga, S. Wolff, B. Hillebrands, and M. P. Kostylev, Appl. Phys. Lett. **94**, 172511 (2009).
[70] K. Yamamoto, G. C. Thiang, P. Pirro, K.-W. Kim, K. Everschor-Sitte, and E. Saitoh, Phys. Rev. Lett. **122**, 217201 (2019).
[71] M. Mohseni, R. Verba, T. Brächer, Q. Wang, D. A. Bozhko, B. Hillebrands, and P. Pirro, Phys. Rev. Lett. **122**, 197201 (2019).
[72] W. F. Brinkman and R. J. Elliott, Proc. R. Soc. A **294**, 343 (1966).
[73] W. Brinkman and R. J. Elliott, J. Appl. Phys. **37**, 1457 (1966).
[74] W. Brinkman, J. Appl. Phys. **38**, 939 (1967).
[75] J. G. Rau, E. K.-H. Lee, and H.-Y. Kee, Phys. Rev. Lett. **112**, 077204 (2014).
[76] B. Bradlyn, J. Cano, Z. Wang, M. G. Vergniory, C. Felser, R. J. Cava, and B. A. Bernevig, Science **353** (2016).
[77] J. Cano, B. Bradlyn, and M. G. Vergniory, APL Mater. **7**, 101125 (2019).
[78] A. Bertin, P. Dalmas de Réotier, B. Fåk, C. Marin, A. Yaouanc, A. Forget, D. Sheptyakov, B. Frick, C. Ritter, A. Amato, C. Baines, and P. J. C. King, Phys. Rev. B **92**, 144423 (2015).
[79] V. K. Anand, A. K. Bera, J. Xu, T. Herrmannsdörfer, C. Ritter, and B. Lake, Phys. Rev. B **92**, 184418 (2015).
[80] K. Tomiyasu, K. Matsuhira, K. Iwasa, M. Watahiki, S. Takagi, M. Wakeshima, Y. Hinatsu, M. Yokoyama, K. Ohoyama, and K. Yamada, J. Phys. Soc. Jpn. **81**, 034709 (2012).

[81] E. Lhotel, S. Petit, S. Guitteny, O. Florea, M. Ciomaga Hatnean, C. Colin, E. Ressouche, M. R. Lees, and G. Balakrishnan, Phys. Rev. Lett. **115**, 197202 (2015).
[82] J. Xu, V. K. Anand, A. K. Bera, M. Frontzek, D. L. Abernathy, N. Casati, K. Siemensmeyer, and B. Lake, Phys. Rev. B **92**, 224430 (2015).
[83] C. Donnerer, M. C. Rahn, M. M. Sala, J. G. Vale, D. Pincini, J. Strempfer, M. Krisch, D. Prabhakaran, A. T. Boothroyd, and D. F. McMorrow, Phys. Rev. Lett. **117**, 037201 (2016).
[84] H. Sagayama, D. Uematsu, T. Arima, K. Sugimoto, J. J. Ishikawa, E. O'Farrell, and S. Nakatsuji, Phys. Rev. B **87**, 100403(R) (2013).
[85] J. Yamaura, K. Ohgushi, H. Ohsumi, T. Hasegawa, I. Yamauchi, K. Sugimoto, S. Takeshita, A. Tokuda, M. Takata, M. Udagawa, M. Takigawa, H. Harima, T. Arima, and Z. Hiroi, Phys. Rev. Lett. **108**, 247205 (2012).
[86] J. N. Reimers, J. E. Greedan, and M. Björgvinsson, Phys. Rev. B **45**, 7295 (1992).
[87] R. Moessner and J. T. Chalker, Phys. Rev. Lett. **80**, 2929 (1998).
[88] J. M. Hastings, L. M. Corliss, and C. G. Windsor, Phys. Rev. **138**, A176 (1965).
[89] J. C. Norvell, W. P. Wolf, L. M. Corliss, J. M. Hastings, and R. Nathans, Phys. Rev. **186**, 557 (1969).
[90] I. A. Kibalin, F. Damay, X. Fabrèges, A. Gukassov, and S. Petit, Phys. Rev. Res. **2**, 033509 (2020).
[91] X. S. Wang, H. W. Zhang, and X. R. Wang, Phys. Rev. Appl. **9**, 024029 (2018).